MFN= 007332
01 SID/SCD
02 5942
03 INPE-5942-PRE/2085
04 MET
05 S
06 as
10 Vadlamudi, Brahmananda Rao
10 Franchito, Sergio Henrique
12 The response of a simple climate model to the sea surface temperature anomalies
14 846-856
30 Annales Geophysicae
31 11
32 9
40 En
41 En
42 <E>
58 DCM
61 <PI>
64 <1993>
68 PRE
76 CIENCIAS METEOROLOGICAS
83 A global two-layer satistical-dynamical primitive equations model is developed to simulate the mean annual conditions and the annual cycle of some zonally averaged atmospheric variables. The model is also used to conduct climatic change experiments related to surface boundary conditions like the sea surface temperature anomalies. The results show that the mean annual conditions and the annual cycle of the zonally averaged atmosphere are reasonably well-simulated. The response of sea surface temperature anomalies for the cases of El Nino, La Nina and the dipole mechanism involving the centers of positive and negative anomalies is studied, In the case of El Nino there is an incrase in the 500 mb temperature and the jet at 250 mb is intensified in both hemispheres. There is also an intendification of the Hadley cell and an increase of the precipitation in the tropical region. The opposite occurs in the case of La Nina. In the experiment considering the dipole case the rising motion in the Hadley cell increases in the northern hemisphere and decreases in the southern hemisphere, and the precipitation is enhanced in the tropical region of the northern hemisphere and reduced in the southern hemisphere.
87 CLIMATOLOGIA DINAMICA
87 MODELOS ATMOSFERICOS
87 ANOMALIA
87 EL NINO
87 LA NINA
87 MUDANCAS CLIMATICAS
90 b
91 FDB-19960515
92 FDB-MLR

Ann. Geophysicae 11, 846–856 (1993)

Annales Geophysicae

The response of a simple climate model to the sea surface temperature anomalies

V. B. Rao, S. H. Franchito

Instituto Nacional de Pesquisas Espaciais, INPE CP 515, 12201 São José dos Campos, SP, Brazil

Received July 10, 1992; revised March 12, 1993; accepted March 29, 1993

Abstract. A global two-layer statistical-dynamical primitive equations model is developed to simulate the mean annual conditions and the annual cycle of some zonally averaged atmospheric variables. The model is also used to conduct climatic change experiments related to surface boundary conditions like the sea surface temperature anomalies. The results show that the mean annual conditions and the annual cycle of the zonally averaged atmosphere are reasonably well-simulated. The response of sea surface temperature anomalies for the cases of El Niño, La Niña and the dipole mechanism involving the centers of positive and negatives anomalies is studied. In the case of El Niño there is an increase in the 500 mb temperature and the jet at 250 mb is intensified in both hemispheres. There is also an intensification of the Hadley cell and an increase of the precipitation in the tropical region. The opposite occurs in the case of La Niña. In the experiment considering the dipole case the rising motion in the Hadley cell increases in the northern hemisphere and decreases in the southern hemisphere, and the precipitation is enhanced in the tropical region of the northern hemisphere and reduced in the southern hemisphere.

1 Introduction

Recently a great deal of effort has been devoted to experiments related to climatic change due to land surface alterations (e.g. Dickinson and Henderson-Sellers, 1988; Shukla *et al.*, 1990; Nobre *et al.*, 1991). Although the General Circulation Models (GCMs) are commonly used for climatic change studies, an efficient way of obtaining some preliminary ideas is employing simplified climate models. Such a model is useful in experiments related to long-term climatic changes, particularly when a large number of experiments is realized. Also, it is doubtful that the GCMs currently in use for climatic change experiments are in fact superior to simpler models used for simulating the global-scale climate feedbacks and the temperature changes (Stone and Risbey, 1990).

Despite the usefulness of simple models only a few tests concerning climatic change have been conducted, particularly regarding the effects of boundary condition modifications, like sea surface temperature (SST) anomalies. For example, Wiin-Nielsen (1986) simulated the simple situation of "El Niño" using a hemispheric statistical-dynamical (SD) quasi-geostrophic model.

Since the earth's climate undergoes significant and grossly predictable seasonal changes, a useful test of the validity of a climate model is its ability to simulate the annual cycle. So, the simplest climatic change experiment is the simulation of the annual cycle. Sela and Wiin-Nielsen (1971) and Wiin-Nielsen (1972) simulated the annual variation of some atmospheric variables using a hemispheric SD quasi-geostrophic model. In the present study, we propose to simulate the annual cycle of the zonally averaged atmosphere using a global SD primitive equations model. We also propose to conduct a series of experiments to investigate the influence on climate caused by SST anomalies. The following cases are considered: a) "El Niño" situation; b) "La Niña" situation; and c) the effects of the dipole mechanism involving the centers of positive and negative anomalies studied by Moura and Shukla (1981), which are known to be related to the occurrence of droughts in northeast Brazil.

2 The model

The model developed is a two-layer SD primitive equations model in sigma-coordinates, similar to that used by Taylor (1980). The model includes parameterizations of friction, diabatic heating and large-scale eddies. However, improvements were made to permit the inclusion of some important climatic processes not previously considered by Taylor (1980) and the model is extended to the southern hemisphere. The effects of latent heat of condensation,

Correspondence to: V. B. Rao

evaporative cooling and subsurface conduction are included. These processes are important in the surface and atmospheric heat balance. The heat fluxes due to surface evaporation and subsurface conduction are parameterized according to Saltzman (1968). The latent heat flux is parameterized following the method of Gutman *et al.* (1984). The other components of atmospheric and surface heating, like the heat fluxes due to shortwave and longwave radiation, and the small-scale convection have functional forms similar to those proposed by Saltzman (1968) and adpated for a two-layer model by Taylor (1980). The parameterization of the diabatic heating is given in Table 1. The meaning of the symbols is the same as in Saltzman (1968) and is indicated in Appendix 1.

The values of the incident radiation flux (R_0) are obtained from the Smithsonian Meteorological Tables (List, 1971). In the model of Taylor (1980) the atmospheric radiative parameters ν_1, ν_2, γ and χ, and the surface albedo (r_s) are fixed, but have different values in each latitude belt. In the present model the atmospheric radiative parameters are considered constant as in Saltzman and Vernekar (1972) ($\nu_1=1.24$, $\nu_2=0.84$, $\gamma=0.95$, and $\chi=0.32$), and the values of the surface albedo are dependent on the type of surface. They are obtained following the procedure described by Saltzman and Vernekar (1972):

$$r_s=j_1\, r_{s\,\text{ocean}}+(j_2+j_4+j_5)\, r_{s\,\text{ice and snow}}+j_3\, r_{s\,\text{land}}, \quad (1)$$

where j_1, j_2 and j_3 are the fractions of the earth's surface covered by ocean, sea ice and land, respectively. The latitudinal distribution of the ocean albedo and the albedo of ice and snow are obtained from Budyko (1958). The land surface albedo is assumed constant (0.2). The fraction covered by ice and snow are divided in two categories: j_4, representing the fraction covered by transient snow, and j_5, corresponding to the part covered by permanent ice and snow.

In the parameterization of the subsurface conduction the factor proportional to the conductive capacity K is considered dependent on the kind of surface, and is determined according to Saltzman and Vernekar (1972):

$$K=j_1\, K_{\text{ocean}}+j_2\, K_{\text{sea ice}}+j_3\, K_{\text{land}}+(j_4+j_5)\, K_{\text{ice and snow}}, \quad (2)$$

where the values of K for each kind of surface are the same as those given by Saltzman and Vernekar (1971) (Table 2).

The values of K^* and G in Table 2 are also the same as those given by Saltzman and Vernekar (1971). $\bar{T}_{DH}$ and $\bar{\theta}_s$ are the zonally averaged subsurface temperature and the potential temperature at the surface of ocean, respectively. The values of $\bar{T}_{DH}$ used in the model are obtained from Saltzman and Vernekar (1972).

The subsurface temperature ($\bar{T}_D$) is calculated as in Saltzman and Vernekar (1971):

$$\bar{T}_D=j_1\, \bar{T}_{DH}+(j_2+j_3+j_4+j_5)\, \bar{T}_{DL}, \quad (3)$$

where $\bar{T}_{DL}$ is the zonally averaged subsurface temperature in the lithosphere. The values of $\bar{T}_{DL}$ used in the model are obtained from Oort (1983).

The latent heat flux is parameterized based on the method proposed by Gutman *et al.* (1984). This method assumes that the precipitation in the latitude belts away from the poles depends on the surface evaporation and the vertical velocity $\bar{\omega}$ (and consequently on the water vapor flux convergence). For a latitude belt near the poles the precipitation depends on the surface evaporation and a correction which depends on the deviation of the cloudiness amount at this latitude belt from its hemispheric average. Considering that the latent heat ($\bar{H}_a$ (4)) and the surface evaporation ($\bar{H}_s$ (4)) fluxes correspond to $L\bar{P}$ and $L\bar{E}$, respectively, the parameterization proposed by Gutman *et al.* (1984) is given by:

$$L\bar{P}=L\bar{E}-L\,a_4\,\bar{\omega}\quad,\ \text{for}\ \phi<70^\circ\text{N} \quad (4)$$
$$L\bar{P}=L\bar{E}+g(N-\bar{N}),\ \text{for}\ \phi>70^\circ\text{N}$$

where L is the latent heat of vaporization; $\bar{P}$ and $\bar{E}$ are the zonally averaged precipitation and evaporation rates; a_4 is a constant obtained by the least square method adjusting the mean annual values of $\bar{\omega}$ (Oort and Rasmusson, 1971); and the values of $(\bar{P}-\bar{E})$ are obtained from Budyko (1978). In the present work we use the $\bar{\omega}$ data from Oort (1983). The value of a_4 obtained was 0.1×10^{-5} m Pa^{-1}. The constant g is determined using the data $(\bar{P}-\bar{E})$ and the deviation of the cloudiness amount at a latitude belt (N) from the hemispheric average ($\bar{N}$) (Sellers, 1965). The values of g used in the model are 238.9 J m^{-2} s^{-1} for the northern hemisphere (Ohring and Adler, 1978; Gutman *et al.*, 1984) and 212 J m^{-2} s^{-1} for the southern hemisphere (Franchito, 1989; Franchito and Rao, 1992).

Equation (4) was proposed by Gutman *et al.* (1984) to parameterize the latent heat flux in the northern hemisphere. Following the same procedure and using the same source of data, Franchito (1989) and Franchito and Rao (1992) suggested the following parameterization for the

Table 1. Functional forms of the diabatic heating at the surface ($\bar{H}_s$) and in the atmosphere ($\bar{H}_a$)

i	$\bar{H}_s(i)$	Parameterization
1	Shortwave solar radiation	$(1-\chi)(1-r_s)(1-r_a)\,R_0$
2	Longwave radiation	$\sigma_B(\nu_1\,\bar{T}_2^4-\bar{T}_s^4)$
3	Small-scale convection	$-b((\bar{T}_s-\bar{T}_3)+c)$
4	Evaporation	$w(e\,\bar{H}_s(3)+f)$
5	Subsurface conduction	$-K(\bar{T}_s-\bar{T}_D)$
i	$\bar{H}_a(i)$	Parameterization
1	Shortwave solar radiation	$\chi(1-r_a)\,R_0$
2	Longwave radiation	$\sigma_B(\gamma\,\bar{T}_s^4-(\nu_1+\nu_2)\,\bar{T}_2^4)$
3	Small-scale convection	$-\bar{H}_s(3)$
4	Latent heat release	Gutman *et al.* (1984)

Table 2. The idealized values of w and k for different surface states

j	Surface state	K (J m^{-2} s^{-1} K^{-1})	w
1	Ocean	$K^*-G(\bar{\theta}_s-\bar{T}_{DH})$	1.00
2	Sea ice	2.42	0.00
3	Land	0.48	0.80
4	Snow and ice	0.48	0.00

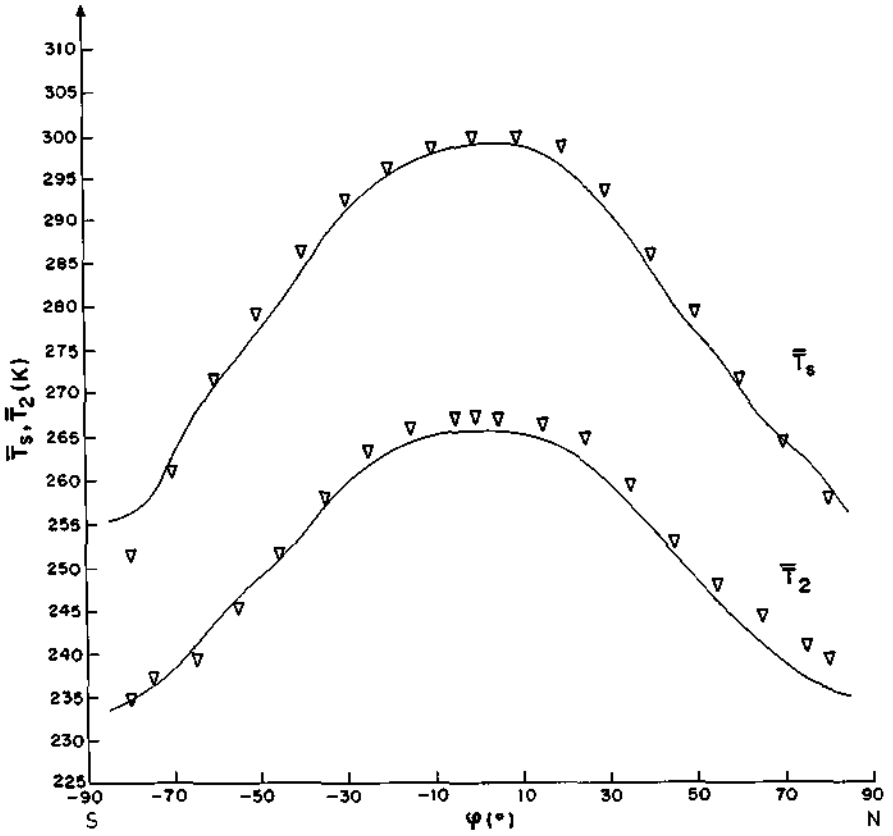

Fig. 1. Latitudinal distribution of the mean annual zonally averaged temperatures (surface and 500 mb). The *solid line* represents the model simulation and the *inverted triangles* indicate the observations (Oort, 1983)

southern hemisphere:

$$L\bar{P} = L\bar{E} - L(a_4\,\bar{\omega} + a_{40}), \text{ for } \phi < 70°\text{S} \quad (5)$$

$$L\bar{P} = L\bar{E} + g\,(N - \bar{N}) \quad , \text{ for } \phi > 70°\text{S},$$

where $a_4 = 0.17 \times 10^{-5}$ m Pa^1, and $a_{40} = 0.2 \times 10^{-8} m\,s^{-1}$.

The computed mean global precipitation is equal to the computed mean global evaporation (within an error limit of 1%).

The expression for the latent heat flux is applied at level 2 (500 mb). The values of this flux for levels 1 and 3 of the present model (250 and 750 mb, respectively) are evaluated considering that they correspond approximately to 10% and 50% of the value at level 2 (Cornejo-Garrido and Stone, 1977).

The initial conditions for the time-integration are: an isothermal atmosphere (270 K) and a state of no motion. The model grid interval is 10° in latitude and the latitudinal centered finite-difference scheme is employed. The equations are time-integrated using an explicit scheme where the time step is 30 min. In order to obtain stability in the integration, the Brown and Campana (1978) and the Asselin filter are used. The model is integrated for 2 years to obtain a stationary solution.

Further details regarding the model can be seen in Franchito (1989).

3 Results

This section is divided into three parts: a. the simulation of the mean annual zonally averaged climate; b. the simulation of the annual cycle; and c. experiments related to sea surface temperature anomalies.

a. Simulation of the mean annual zonally averaged climate

The results concerning the mean annual zonally averaged climate are fundamentally the same as those shown in Franchito and Rao (1992). However, in the present paper we do not consider the biofeedback mechanism which links the surface state to the atmosphere as in the previous paper. Here we are interested in the climatic changes due to SST anomalies, so we use a simpler parameterization of the evaporation based on Saltzman (1968), as shown in Table 1. Despite this simplification the model produces similar results regarding the characteristics of mean annual zonally averaged climate. This will be shown below.

Figures 1–4 show the simulations of the zonally averaged temperatures (surface and 500 mb), zonal wind (250 and 750 mb), vertical velocity at 500 mb, and precipitation, respectively. The observed data are taken from Oort (1983) (Figs. 1–3) and from Schutz and Gates (1971, 1972, 1973, 1974) (Fig. 4).

It can be noted in Fig. 1 that the latitudinal profiles of the temperatures are successfully simulated. The maximum deviations of the computed temperature from the observations occur near the poles and are of the order of 4 °C. In general, the temperature deviations at the two levels are in the same direction, so the temperature difference between the surface and 500 mb is better simulated.

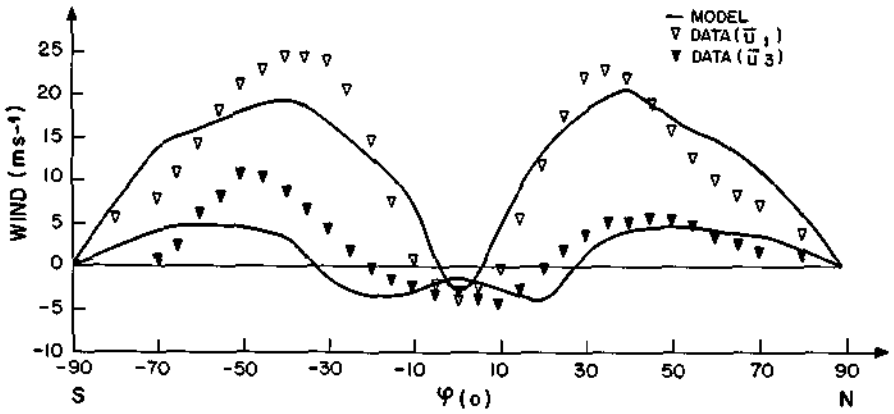

Fig. 2. Latitudinal distribution of the mean annual zonally averaged zonal winds at 250 ($\bar{u}_1$) and 750 mb ($\bar{u}_3$). The *solid line* represents the model simulation. The observations of $\bar{u}_1$ ($\bar{u}_3$) are indicated by *full (empty) inverted triangles* (Oort, 1983)

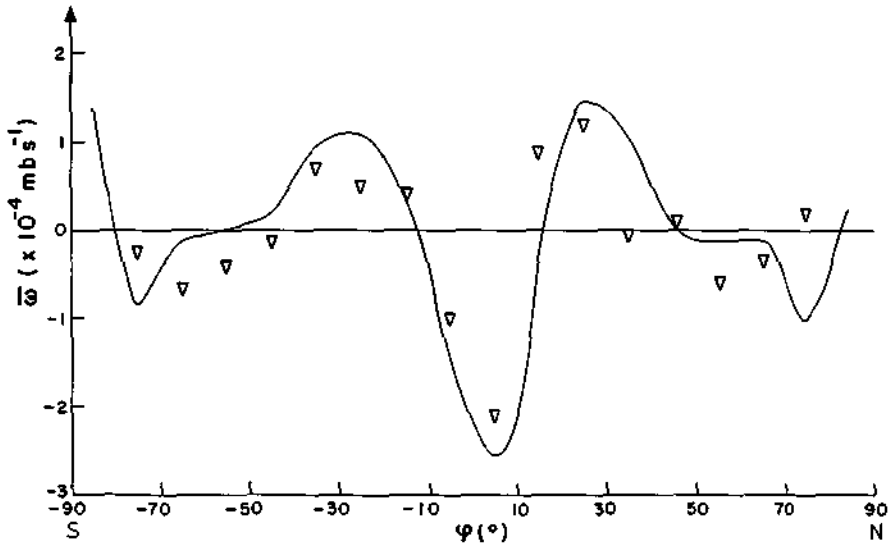

Fig. 3. Latitudinal distribution of the mean annual zonally averaged vertical velocity at 500 mb. The *solid line* represents the model simulation and the *inverted triangles* indicate the observations (Oort, 1983)

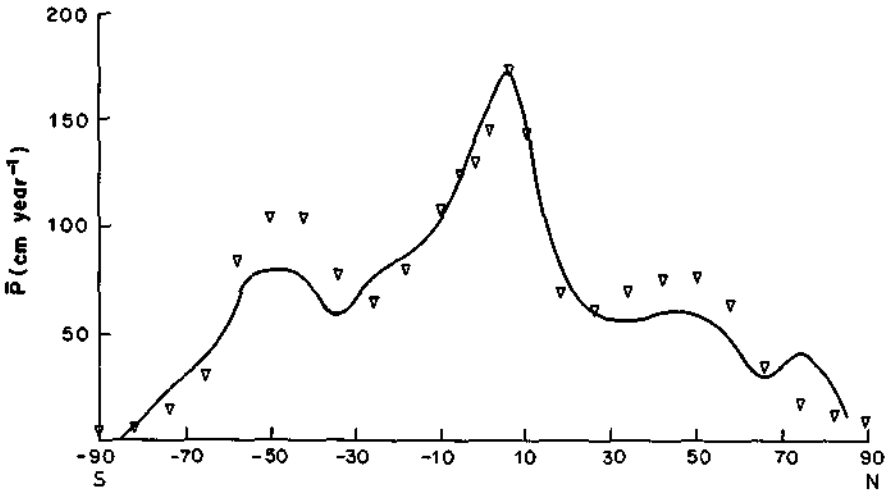

Fig. 4. Latitudinal distribution of the mean annual zonally averaged precipitation. The *solid line* represents the model simulation and the *inverted triangles* indicate the observations (Schutz and Gates, 1971, 1972, 1973, 1974)

Figure 2 shows the latitudinal profiles of the zonal wind. It can be seen that the general form of the curves is well-simulated. The simulation is better for the case of the 250 mb zonal wind. The values simulated in the equatorial region are very close to the observed values and the positions of the maxima are well-simulated, although they are shifted slightly poleward. However, the magnitudes of the zonal wind are smaller than the observed values mainly in the southern hemisphere. The latitudinal variation of the zonal wind at 750 mb is well-simulated in the northern hemisphere, but the peak is underestimated in the southern hemisphere.

The latitudinal variation of the vertical velocity at 500 mb is shown in Fig. 3. The three cells of the mean meridional circulation can be seen: the ascending and the descending branches of the Hadley cell; the subsidence

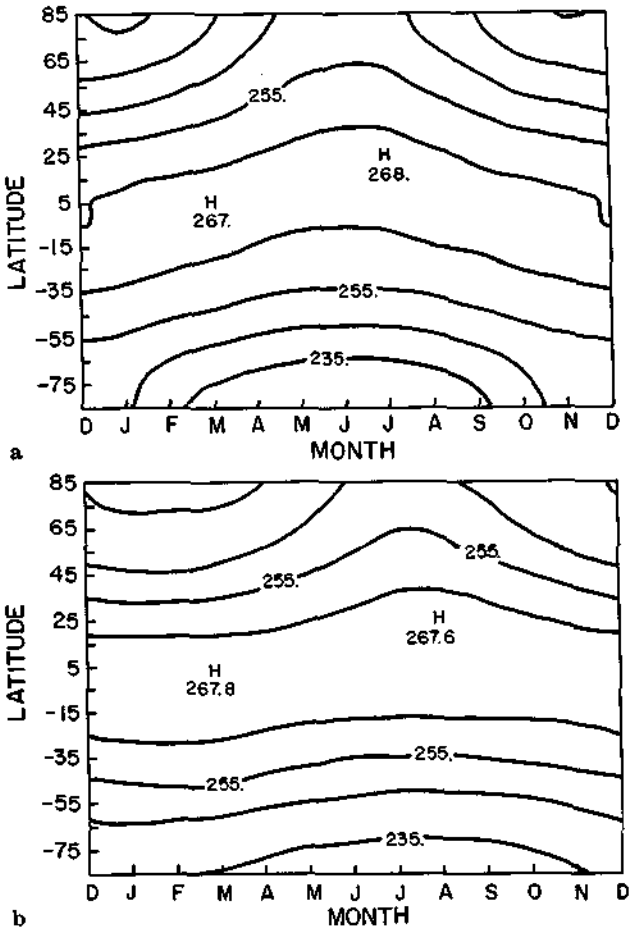

Fig. 5a,b. Latitudinal distribution of the annual variation of the zonally averaged temperature at 500 mb: **a** simulated; and **b** observed. (Oort, 1983). The contour interval is 10 K

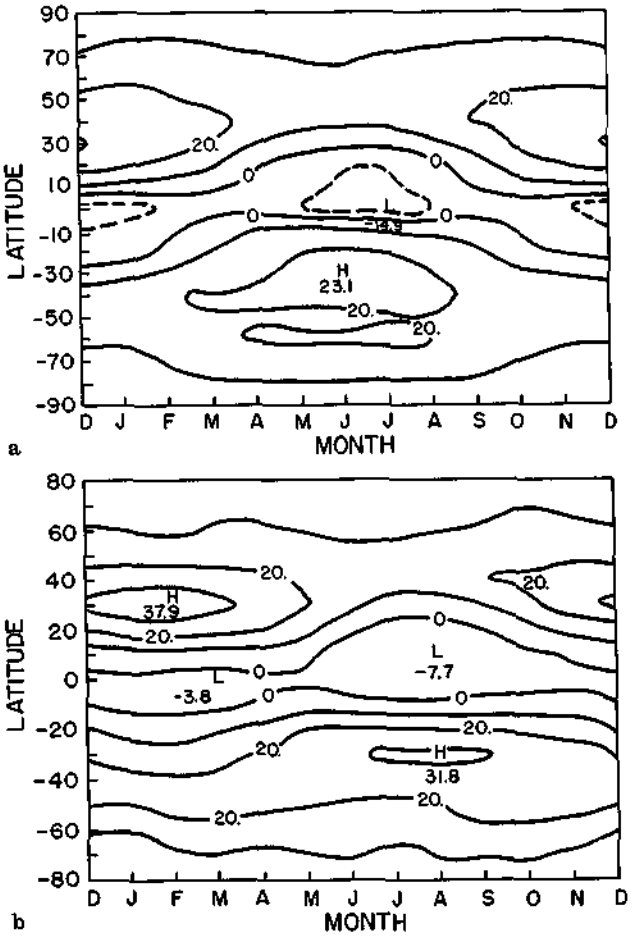

Fig. 6a,b. Latitudinal distribution of the zonally averaged zonal wind at 250 mb: **a** simulated; and **b** observed (Oort, 1983). The contour interval is 10 m s^{-1}

zone between 15°–45°N(S); the convergence zone in temperature latitudes; and also a region of ascending motion near the poles. The magnitude and position of the maximum of the ascending movement in the Hadley cell are well-simulated. The maximum is situated at 5°N which coincides with the mean position of the equatorial trough (Riehl, 1954).

The general form of the latitudinal variation of the precipitation is well-simulated (Fig. 4). The agreement between the simulation and observations is good in the region 30°S–30°N, and the position and magnitude of the maximum are very well-simulated. This is due to the fact that the Hadley cell was successfully reproduced, as shown in Fig. 3. The secondary maxima of the precipitation are underestimated because the principal precipitation process in these regions is related to the meridional transport of water vapor by baroclinic eddies, which is not included in the model.

b. Simulation of the annual cycle

In order to simulate the annual cycle, latitudinal distributions of R_0 and T_D for each month are used. A simple linear interpolation formula was used to obtain these values at 3-day intervals in the integration of the zonally averaged equations. Since we are interested in simulating the annual variation, the model is integrated for a period of 3 years, where the first 2 years correspond to the period necessary to obtain the adjustment of the variables. The initial data is 1 January and the results presented correspond to the third year of integration.

Figure 5 shows the simulated and observed annual variation of the 500-mb zonally averaged temperature. As can be noted, there is a good agreement between the simulated and observed values. The position and the magnitude of the maxima are well-simulated, although the maximum occurs earlier in the simulation compared to the observations in the northern hemisphere. The amplitude of the annual cycle is closer to the observations than the results obtained by Sela and Wiin-Nielsen (1971). They found a large annual variation of most quantities, probably due to the simplicity of the thermal forcing.

In Fig. 6, the simulated and observed annual variation of the zonally averaged zonal wind at 250 mb is presented. Again, a good agreement is noted between the simulation and observations. The positions of the maxima are well-simulated in both hemispheres, although the magnitudes are somewhat lower than the observed values. It is also seen that the region of easterlies near the equator is

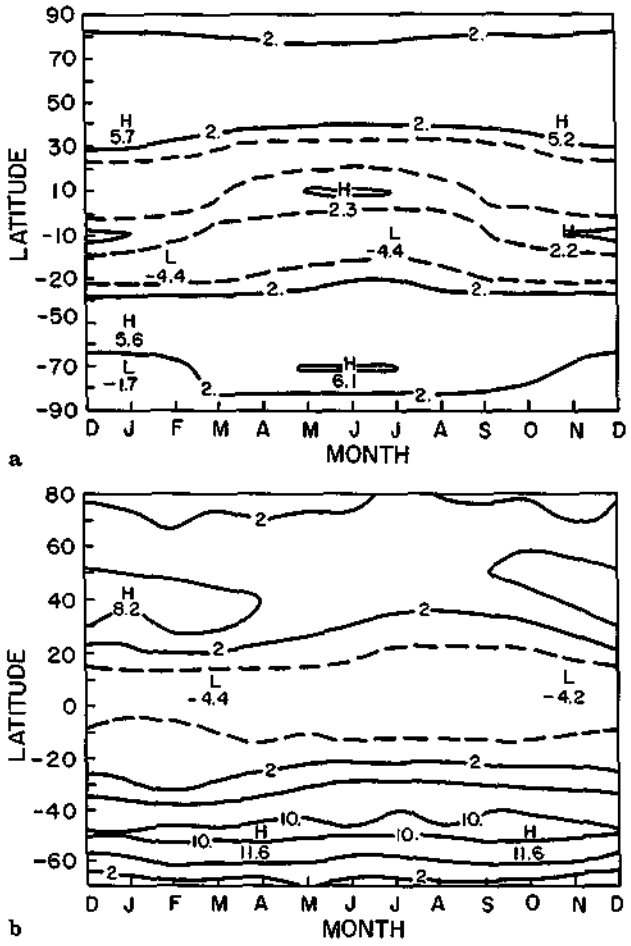

Fig. 7a,b. Latitudinal distribution of the zonally averaged zonal wind at 750 mb: a simulated; and b observed (Oort, 1983). The contour interval is 4 m s^{-1}

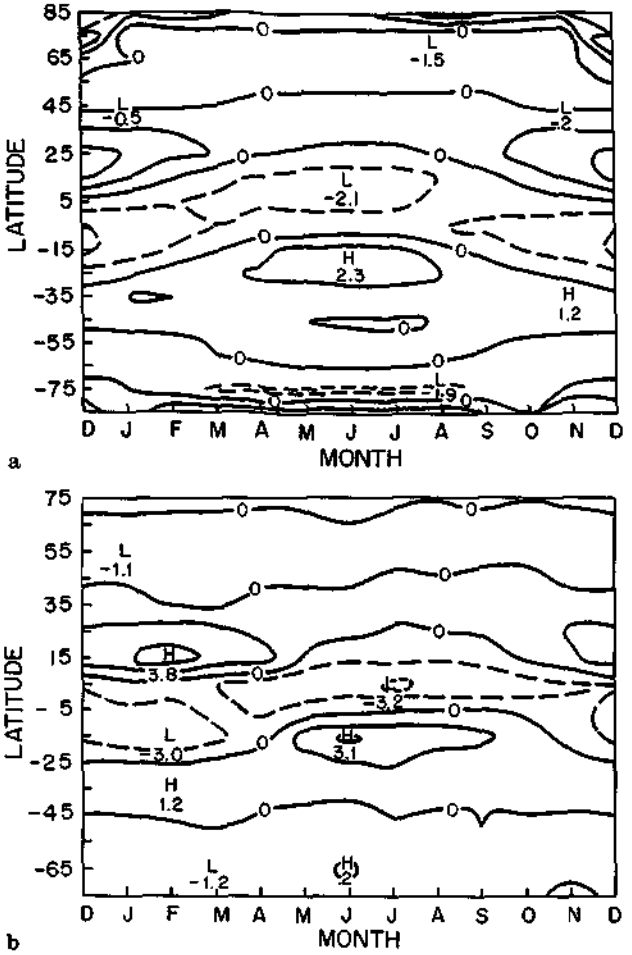

Fig. 8a,b. Latitudinal distribution of the zonally averaged vertical velocity at 500 mb: a simulated; and b observed (Oort, 1983). The countour interval is 1×10^{-4} mb s^{-1}

well-simulated, but the winds are stronger than the observations. The annual variation of the 250-mb zonal wind at higher latitudes is better simulated in our model than by Sela and Wiin-Nielsen (1971), where a region of easterlies (not observed) occurred in the northern hemisphere summer.

Figure 7 shows the simulated and observed annual variation of the zonally averaged zonal wind at 750 mb. The regions of the maximum are well-simulated in the northern hemisphere. The latitude belt containing the stronger winds is shifted poleward in the southern hemisphere. The region of easterlies in the tropics is relatively well-simulated, although there is a small region of westerlies (not observed) in the northern hemisphere summer. Our results for the amplitude of the annual variation of the 750-mb zonal winds agree better with observations than those of Sela and Wiin-Nielsen (1971). Also, we do not find a region of easterlies in the high latitudes which appears in their results.

The annual cycle of the vertical velocity ($\bar{\omega}$) is shown in Fig. 8. As can be seen, there is a good agreement between the simulation and the observations: the Hadley cell is stronger in winter and it penetrates into the summer hemisphere. This cell is weaker in the summer hemisphere and it is situated in a region away from the equator. The annual variation of the other cells is also reasonably well-simulated.

Table 3. Anomalies of SST used in the "El Niño", "La Niña", and "dipole" experiments

Latitude	"El Niño" $\bar{T}_{DH}$ (K)	"La Niña" $\bar{T}_{DH}$ (K)	Dipole $\bar{T}_{DH}$ (K)
25°N			0.5
15°N	0.5	1.0	2.0
5°N	2.0	−4.0	1.5
5°S	4.0	−4.0	−1.0
15°S	2.0	1.0	−2.0
25°S	−1.5		−1.0

c. *The response to sea surface temperature anomalies*

The experiments carried out considering the case of SST anomalies are: a) "El Niño" situation (Experiment 1); b) "La Niña" situation (Experiment 2); and c) dipole case (Experiment 3). The SST anomalies used in the three ex-

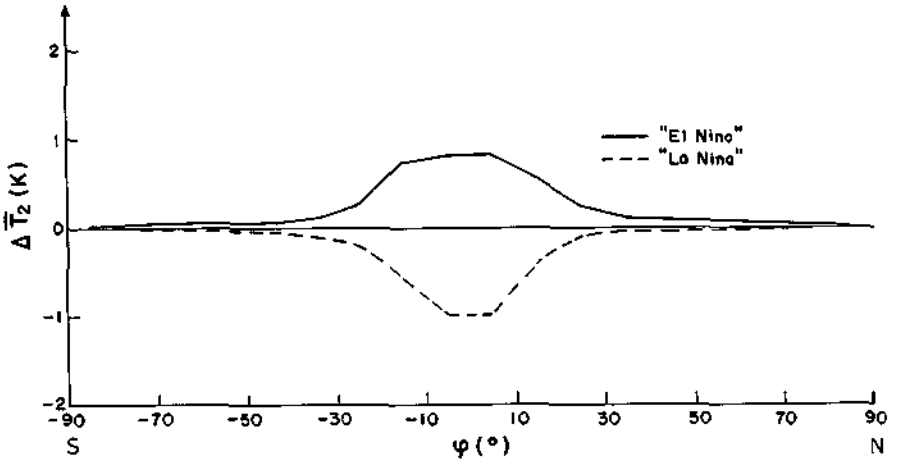

Fig. 9. Changes (perturbed minus control) in the 500-mb zonally averaged temperature in the "El Niño" (*solid line*) and "La Niña" (*dashed line*) experiments

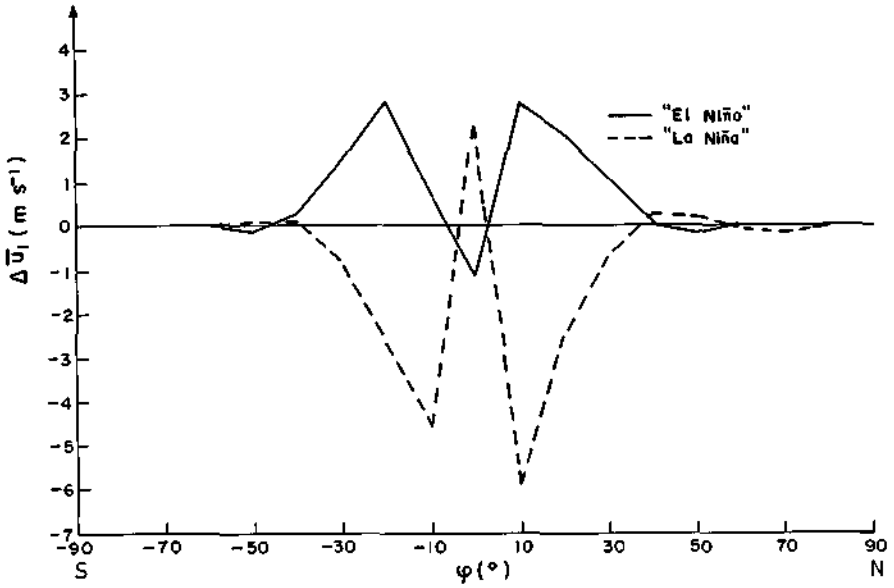

Fig. 10. As in Fig. 9 but for the 250-mb zonally averaged zonal wind

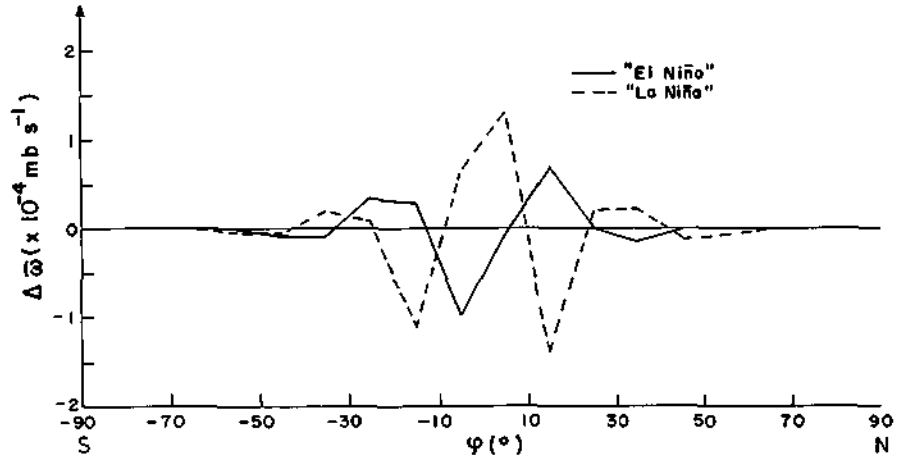

Fig. 11. As in Fig. 9 but for the zonally averaged vertical velocity at 500 mb

periments were obtained from the Oceanographic Monthly Summary (1983) and are given in Table 3. The results are given in terms of a perturbed minus control case (simulation of the mean annual zonally averaged atmosphere).

The principal results of Experiments 1 and 2, regarding the zonally averaged characteristics, such as the 500 mb temperature, zonal wind at 250 mb, vertical velocity, evaporation and precipitation, are presented in Figs. 9–13, respectively. The most notable deviations occur in the perturbed areas. In Experiment 1, there is an increase in the 500-mb temperature, with the largest variation occurring in the region where the source of anomalies is strongest (Fig. 9). As a consequence of the thermal

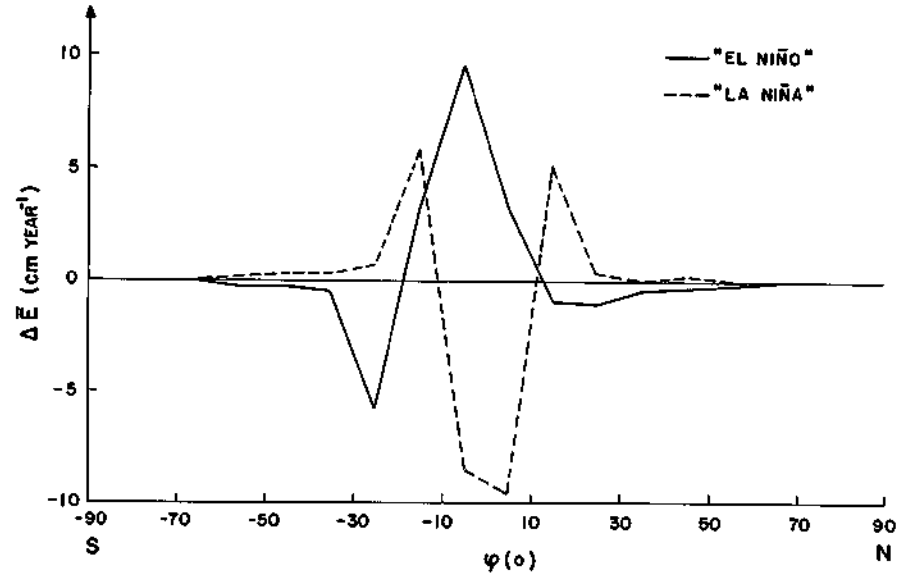

Fig. 12. As in Fig. 9 but for the zonally averaged evaporation

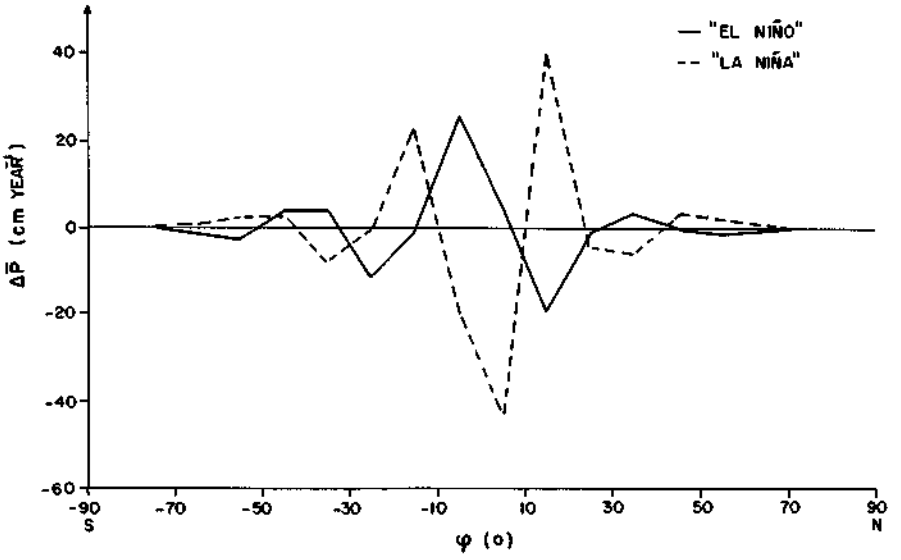

Fig. 13. As in Fig. 9 but for the zonally averaged precipitation

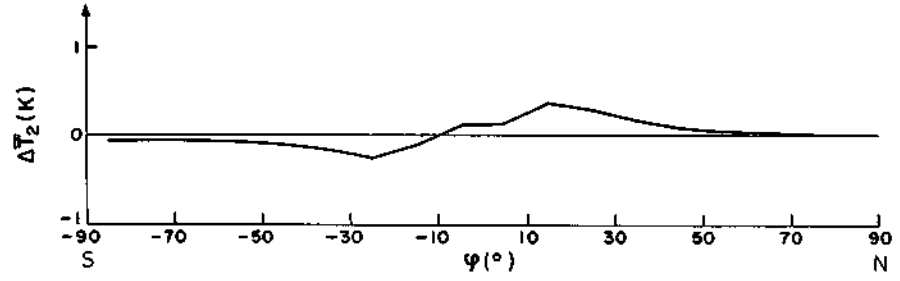

Fig. 14. Changes (perturbed minus control) for the 500-mb zonally averaged temperature in the "dipole" experiment

wind balance, the zonal wind is intensified in both hemispheres with the largest variation occurring in the latitude belts immediately to the north (south) from the perturbed area in the northern (southern) hemisphere (Fig. 10). There is an intensification of the Hadley cell and an increase in evaporation (Figs. 11 and 12, respectively) and consequently there is an increase in the precipitation in the tropical region (Fig. 13). The opposite is observed in Experiment 2: there is a decrease in the intensity of the zonal wind at 250 mb and in the 500-mb temperature in the perturbed zone. The Hadley cell is weak and the evaporation decreases, and so the precipitation is reduced in the equatorial region.

Observational studies (Kayano *et al.*, 1989) indicate that the El Niño/La Niña events change the Walker circulation. With the present model these cannot be studied. However, important changes do also occur in the zonally averaged parameters which are well-simulated by the model, as shown above.

The principal results of Experiment 3 regarding the zonally averaged variables – 500-mb temperature, zonal wind at 250 mb, vertical velocity, evaporation and precip-

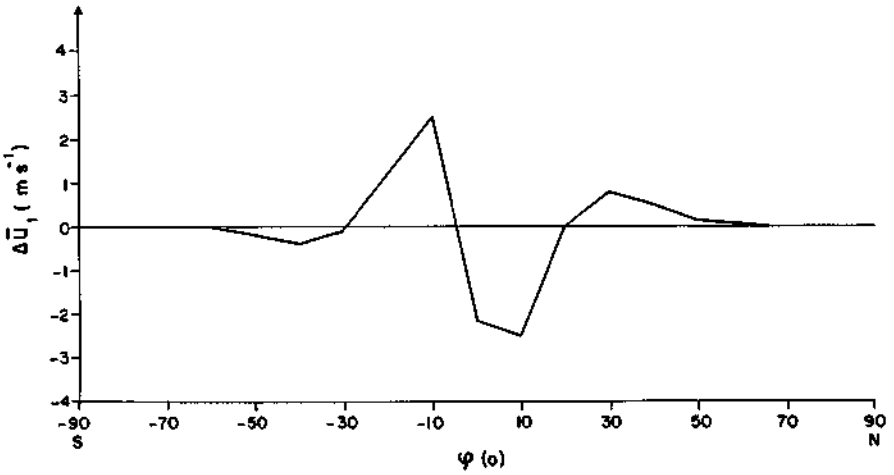

Fig. 15. As in Fig. 14 but for the zonally averaged zonal wind at 250 mb

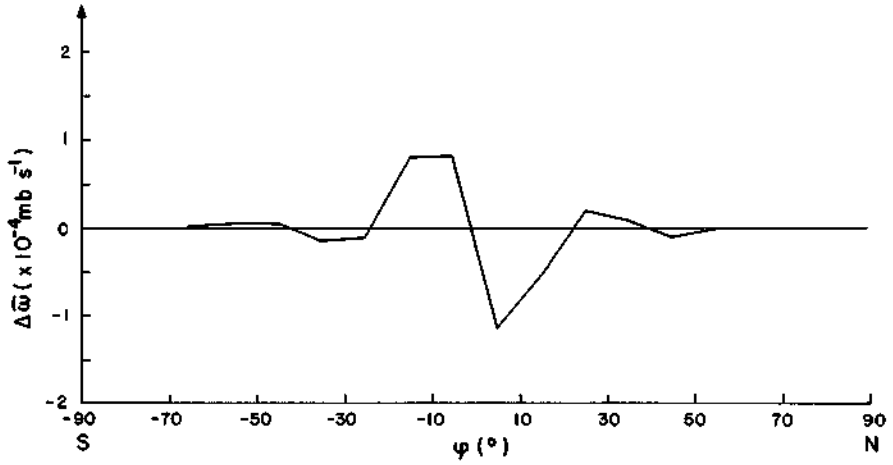

Fig. 16. As in Fig. 14 but for the zonally averaged vertical velocity at 500 mb

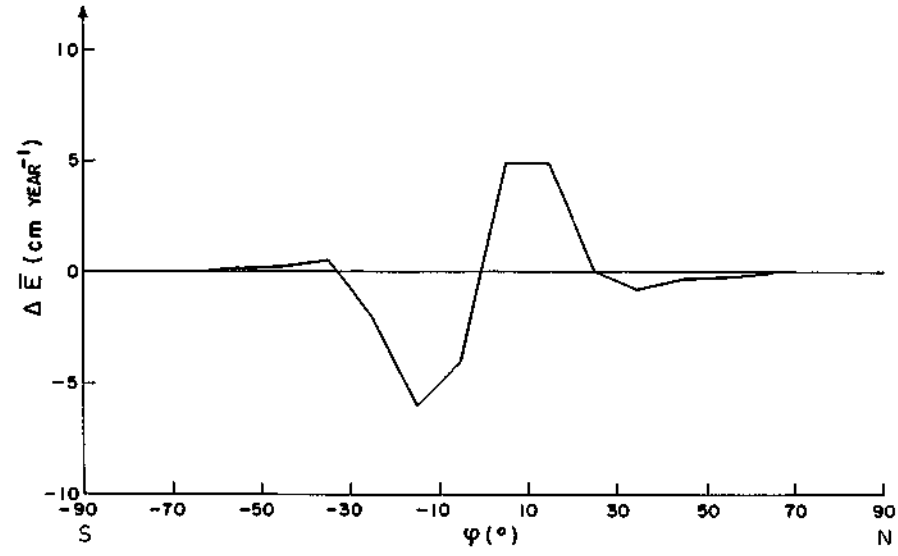

Fig. 17. As in Fig. 14 but for the zonally averaged evaporation

itation – are shown in Figs. 14–18, respectively. The 500 mb temperature increases (decreases) northward (southward) from 10°S, with the largest variation occurring in the area where the source is strongest (Fig. 14). As can be noted in Fig. 15, the zonal wind at 250 mb increases northward from the maximum of the source in the northern hemisphere. In the southern hemisphere the largest increase also occurs northward of the region where the source is more intense. The rising motion in the Hadley cell increases in the northern hemisphere and decreases in the southern hemisphere (Fig. 16), and the same occurs with the evaporation (Fig. 17). This means that there is an enhancement in the precipitation in the tropical region of the northern hemisphere and a reduction in

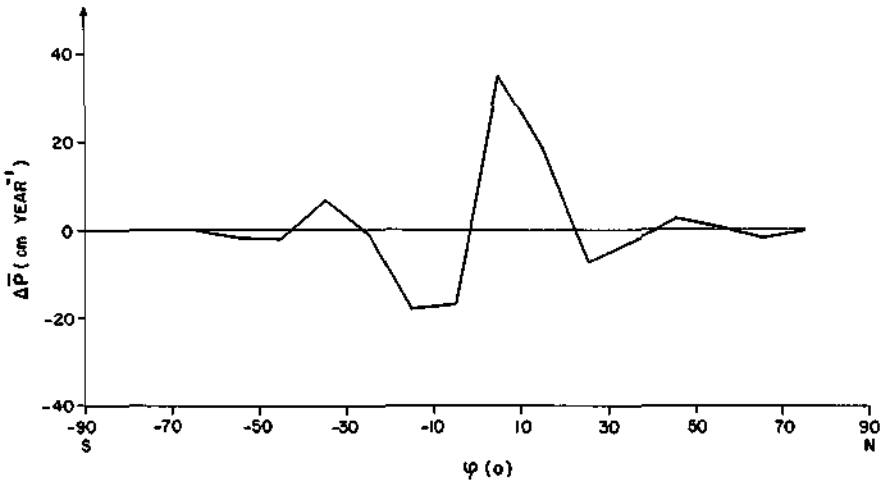

Fig. 18. As in Fig. 14 but for the zonally averaged precipitation

the southern hemisphere (Fig. 18). These results agree with those given by Moura and Shukla (1981), which are obtained using a sophisticated GCM model.

4 Conclusion

In this paper the usefulness of simple models in climatic change experiments is investigated. A two-layer statistical-dynamical model is developed with the twofold purpose of simulating the annual mean and the annual variation of some zonally averaged atmosphere characteristics, and studying the climatic response to surface boundary conditions modifications, particulary the response to sea surface temperature anomalies ("El Niño", "La Niña", and dipole cases).

The results show that the model simulates reasonably well the mean annual and the annual variations of some characteristics of the zonally averaged atmosphere, such as the 500 mb temperature, the zonal winds at 250 and 750 mb, and the mean meridional circulation. The purpose of simulating the annual cycle is to consider the simplest case of climate change. In the experiments related to the response to sea surface temperature anomalies, the model simulates accurately some of the climatic effects that are observed in those situations. In the case of "El Niño" experiment there is an intensification of the zonal wind at 250 mb and of the Hadley cell, and the precipitation increases in the tropical region. The opposite situation occurs in the "La Niña" experiment. In the dipole case the ascending branch of the Hadley cell is intensified in the northern hemisphere and weakened in the southern hemisphere; the evaporation and the precipitation increase (decrease) in the tropical zone of the northern (southern) hemisphere.

Thus the simple climate model developed here is a useful tool in performing experiments related to climatic change, mainly for obtaining the preliminary and qualitative ideas regarding the effects such as "El Niño", "La Niña", and dipole. Also, several studies of climatic change could be undertaken with this simple model in future. For example, the model might be useful for conducting numerical experiments considering the climatic effects due to land surface alterations, modifications in the radiative parameters, alterations in the amount of ice in a latitude belt and many others.

Acknowledgements. Thanks are due to Miss Roselira P. da Silva for typing.

Appendix 1. List of symbols

a_4	constant in equation: 0.1×10^{-5} m Pa^{-1} (HN) and 0.17×10^{-5} m Pa^{-1} (HS)
a_{40}	constant in equation: 0.2×10^{-8} m s^{-1}
b, c, e, f, g	empirical constants independent of the latitude
$\bar{E}$	zonally averaged evaporation
$\bar{H}_a(i)$	diabatic heating of the atmosphere
$\bar{H}_s(i)$	heat transfer at the surface
i	index indicating the physical process in $\bar{H}_s(i)$ and $\bar{H}_a(i)$ in Table 1.
K	factor proportional to the conductive capacity of surface medium.
K^*	value of K for the ocean
L	latent heat of vaporization
N	cloudiness amount at a latitude belt
$\bar{N}$	hemispheric average of the cloudiness amount
$\bar{P}$	zonally averaged precipitation
r_a	albedo of the atmosphere
r_s	surface albedo
$\bar{T}_D$	subsurface temperature
$\bar{T}_{DH}$	subsurface temperature of ocean
$\bar{T}_{DL}$	subsurface temperature in lithosphere
$\bar{T}_s$	surface temperature
$\bar{T}_2$	temperature at 500 mb
w	water availability parameter
ϕ	latitude
γ	longwave absorptivity of atmosphere
χ	opacity of the atmosphere to solar radiation
ν_1, ν_2	factors for downward and upward effective blackbody longwave radiation
σ_B	the Stefan-Boltzman constant
$\bar{\omega}$	vertical velocity
$\bar{\theta}_s$	zonally averaged potential temperature at the surface

References

Brown, J. A., and K. A. Campana, An economical time-differencing system for numerical weather prediction, *Mon. Weather Rev.*, **106,** 1125–1136, 1978.

Budyko, M. I., The heat balance of the earth's surface, pp 35–40, US Weather Bureau, Washington, D.C., 1958.

Cornejo-Garrido, A. G., and P. H. Stone, On the heat balance of the Walker circulation, *J. Atmos. Sci.*, **34,** 1155–1162, 1977.

Dickinson, R. E., and A. Henderson-Sellers, Modeling tropical deforestation: a study of GCM land surface parameterizations, *Q. J. R. Meteorol. Soc.*, **114,** 439–462, 1988.

Franchito, S. H., Numerical experiments with zonally averaged climate models, *Ph. D. Thesis,* Instituto Nacional de Pesquisas Espaciais, INPE, 1989. (Available from INPE, CP 515, 12201-970, São José dos Campos, SP, Brazil).

Franchito, S. H., and V. B. Rao, Climatic change due to land surface alterations, *Clim. Change,* **22,** 1–34, 1992.

Gutman, G., G. Ohring and J. H. Joseph, Interaction between the geobotanic state and climate: a suggested approach and a test with a zonal model, *J. Atmos. Sci.*, **41,** 2663–2678, 1984.

Kyano, M. T., V. B. Rao and A. D. Moura, The Walker circulation and atmospheric water vapor characteristics over the Pacific for two contrasting years, *Int. J. Climatol.*, **9,** 243–251, 1989.

List, R. J., Smithsonian Meteorological Tables, 6th revised edn., Smithsonian Institute, Washington, D.C., 1971.

Moura, A. D., and J. Shukla, On the dynamics of droughts in northeast Brazil: observations, theory and numerical experiments with a general circulation model, *J. Atmos. Sci.*, **38,** 2653–2675, 1981.

Nobre, C. A., P. Sellers, and J. Shukla, Amazonian deforestation and regional climate change, *J. Climate,* **4,** 957–988, 1991.

Oceanographic Monthly Summary, Department of Commerce, NOAA, Washington, 1983.

Ohring, G., and S. Adler, Some experiments with a zonally averaged climate model, *J. Atmos. Sci.*, **35,** 186–205, 1978.

Oort, A. H., Global Atmospheric Circulation Statistics, *NOAA Prof. Pap. 5,* 1983.

Oort, A. H., and E. M. Rasmusson, Atmospheric Circulation Statistics, *NOAA Prof. Pap. 5,* 1971.

Riehl, H., *Tropical Meteorology,* McGraw-Hill, New York, 1954.

Saltzman, B., Steady-state solutions for axially symmetric climate variables, *Pure Appl. Geophys.*, **69,** 237–259, 1968.

Saltzman, B., and A. D. Vernekar, An equilibrium solution of the axially symmetric component of the earth's macroclimate, *J. Geophys. Res.*, **76,** 1498–1524, 1971.

Saltzman, B., and A. D. Vernaker, Global equilibrium solutions for the zonally averaged macroclimate, *J. Geophys. Res.*, **77,** 3936–3945, 1972.

Schutz, C., and W. L. Gates, Global climatic data for surface, 800 mb, 400 mb: January, *R-915-ARPA,* Rand Corporation, Santa Monica, Calif., 1971.

Schultz, C., and W. L. Gates, Global climatic data for surface, 800 mb, 400 mb: July, *R-1029-ARPA,* Rand Corporation, Santa Monica, Calif., 1972.

Schultz, C., and W. L. Gates, Global climatic data for surface, 800 mb, 400 mb: April, *R-1317-ARPA,* Rand Corporation, Santa Monica, Calif., 1973.

Schultz, C., and W. L. Gates, Global climatic data for surface, 800 mb, 400 mb: October, *R-1425-ARPA,* Rand Corporation, Santa Monica, Calif., 1974.

Sela, J. and A. Wiin-Nielsen, Simulation of the atmospheric annual energy cycle, *Mon. Weather Rev.*, **99,** 460–468, 1971.

Sellers, W. D., *Physical Climatology,* University of Chicago Press, Chicago, Ill., 1965.

Shukla, J., C. A. Nobre, and P. J. Sellers, Amazonian deforestation and climate change, Science, **247,** 1322–1325, 1990.

Stone, P. H., and J. S. Risbey, On the limitations of general circulation climate models, *Geophys. Res. Lett.*, **17,** 2173–2176, 1990.

Taylor, K. E., The roles of mean meridional motions and large-scale eddies in zonally averaged circulations, *J. Atmos. Sci.*, **37,** 1–19, 1980.

Wiin-Nielsen, A., Simulation of the annual variation of the zonally averaged state of the atmosphere, *Geofis. Publ. Geophys. Norvegica,* **28,** 1–45, 1972.

Wiin-Nielsen, A., On simple estimates of the impact of heating anomalies on the zonal atmospheric circulation, *Ann. Geophysicae,* **4,** 365–376, 1986.